Supplementary Information

A. LINK PERFORMANCE OVER TIME (MAIN TEXT FIG. 3)

The parameters of the measurement illustrated in Fig. 3 of the main text are listed in Supplementary Table 1, where N_{A} and N_{B} are the number of measured photon detections, $N_{\mathrm{s}}^{\mathrm{z}}$ and $N_{\mathrm{s}}^{\mathrm{x}}$ are the sifted key lengths and E_{μ}^{z} and E_{μ}^{x} are the extracted quantum bit error rates in the z and x basis respectively.

Supplementary Table 1. Experimental parameters of data illustrated in Fig. 3 of the main text

Time (s)	N_{A}	N_{B}	$N_{\mathrm{s}}^{\mathrm{z}}$	$N_{\mathrm{s}}^{\mathrm{x}}$	E_{μ}^{z} (%)	E_{μ}^{x} (%)	Secure key rate (bps)
68	891312444	442055	12100	17960	6.595	7.0657	71.7972

B. SECURE KEY RATES FOR DIFFERENT LOSSES (MAIN TEXT FIG.4)

Here, additional experimental parameters of the measurement used in Fig. 4 of the main text are provided. They are listed in Supplementary Table 2, where η_{A} is the heralding efficiency and R_{A} is the single photon rate of the source after single-mode coupling for Alice's channel, e_{d} is the misalignment error rate, τ_{cw} is the coincidence window and $Y_{0\mathrm{A}}$ and $Y_{0\mathrm{B}}$ are the dark count rates per coincidence window for Alice and Bob respectively.

Supplementary Table 2. Experimental parameters of data illustrated in Fig. 4 of the main text

η_{A} (%)	$R_{\mathrm{A}}(s^{-1})$	e_{d} (%)	$Y_{0\mathrm{A}}$	$Y_{0\mathrm{B}}$	τ_{cw} (ns)
31.42	1.57×10^7	3.3	4.71×10^{-4}	2.2×10^{-6}	1.0

C. SECURE KEY RATE FOR DIFFERENT PHOTON PAIR RATES (MAIN TEXT FIG. 5)

In Fig. 5 of the main text we study the influence of the photon pair rate emitted by the source on the secure key rate under different channel losses. The photon pair rate per coincidence window μ is calculated via

$$\mu = \frac{R_{\mathrm{A}} - Y_{0\mathrm{A}}/\tau_{\mathrm{cw}}}{\eta_{\mathrm{A}}} \tau_{\mathrm{cw}} \tag{1}$$

from experimental data. We use 5 measurements to demonstrate the influence of the photon pair rate on the extracted secure key rate. The most relevant parameters of these measurements are listed in Supplementary Table 3.

Supplementary Table 3. Experimental parameters for different measurements illustrated in Fig. 5 of the main text

Total Time (s)	μ	Channel Loss (dB)	$N_{\mathrm{s}}^{\mathrm{z}}$	$N_{\mathrm{s}}^{\mathrm{x}}$	E_{μ}^{z}	E_{μ}^{x}	Secure key rate (bps)
15	0.0402	43.52	6062	8973	0.057737	0.057617	300.865
131	0.0151	43.75	19110	26719	0.027316	0.077772	114.9127
85	0.0493	46.89	20066	29351	0.059653	0.063269	153.526
57	0.0402	48.44	7846	11646	0.065893	0.066632	77.07702
100	0.0673	49.56	17311	25885	0.080065	0.080471	48.733

D. DUAL DOWNLINK FROM A LEO (MAIN TEXT FIG. 6)

We investigated the achievable secure key rate in a dual downlink scenario from a low earth orbit (LEO) in Fig. 6 of the main text. The dark count rate Y_0 of the detectors, which takes care of both after-pulsing from avalanche photo diodes and accidental coincidence counts is given by $Y_0 = \mu\eta P_{\mathrm{a}} + \tau_{\mathrm{cw}} R_{\mathrm{DC}}$, where η is the overall detection efficiency,

P_a is the after-pulsing probability and R_{DC} is the accidental count rate of the detectors. In accordance with the measurements on our free-space link, we choose this parameters as $P_a = 3.0\,\%$, $R_{DC} = 1000\,\text{cps}$ and $e_d = 1.5\,\%$. The standard deviation of the coincidence histogram is assumed to be 770 ps, and in accordance with the "Micius" dual downlink experiment [1] we choose a coincidence window of $\tau_{cw} = 2.5\,\text{ns}$. With a heralding efficiency of 30 %, the entangled source on "Micius" produces photon pairs at a rate of 5.9 MHz, which corresponds to a photon pair rate per coincidence window of $\mu_{\text{Micius}} = 0.0492$.

E. OPTIMAL PAIR RATE FOR A DUAL DOWNLINK SCENARIO WITH SNSPDS

In the Discussion section of the main text we mention the optimal pair rate in a dual downlink scenario assuming that the ground stations are equipped with superconducting nanowire single-photon detectors (SNSPDs). The optimal pair rate of 814 Mcps is calculated using the link specifications listed in Supplementary Table 4.

Supplementary Table 4. Typical parameters of SNSPDs used to estimate the optimal pair rate

Total channel loss (dB)	Detector dead-time (ns)	Y_{0A}/Y_{0B}	Timing jitter (ps)	τ_{cw} (ps)
70	25	3.3×10^{-9}	20	66.6

F. SKY NOISE OF A TYPICAL LEO SATELLITE PASS

We measured the background noise of the night sky with the same detection module used for our terrestrial free-space link. The module is mounted on the Ritchey-Chrétien reflector telescope of the optical ground station with a primary aperture of 1 m, which followed a polar satellite orbit, depicted in Supplementary Fig. 1b). In order to reduce the sky noise, an interference filter with a FWHM bandwidth of 3 nm and a long pass filter were mounted in front of each detector. All detectors had a field of view of 300 μrad at FWHM. In Supplementary Fig. 1a) the summed up sky noise of all four detector channels is illustrated, with detector dark counts subtracted. The simulated satellite pass started at an elevation angle of 8°, went up to 40° at the closest approach and was terminated at the descend at 5°.

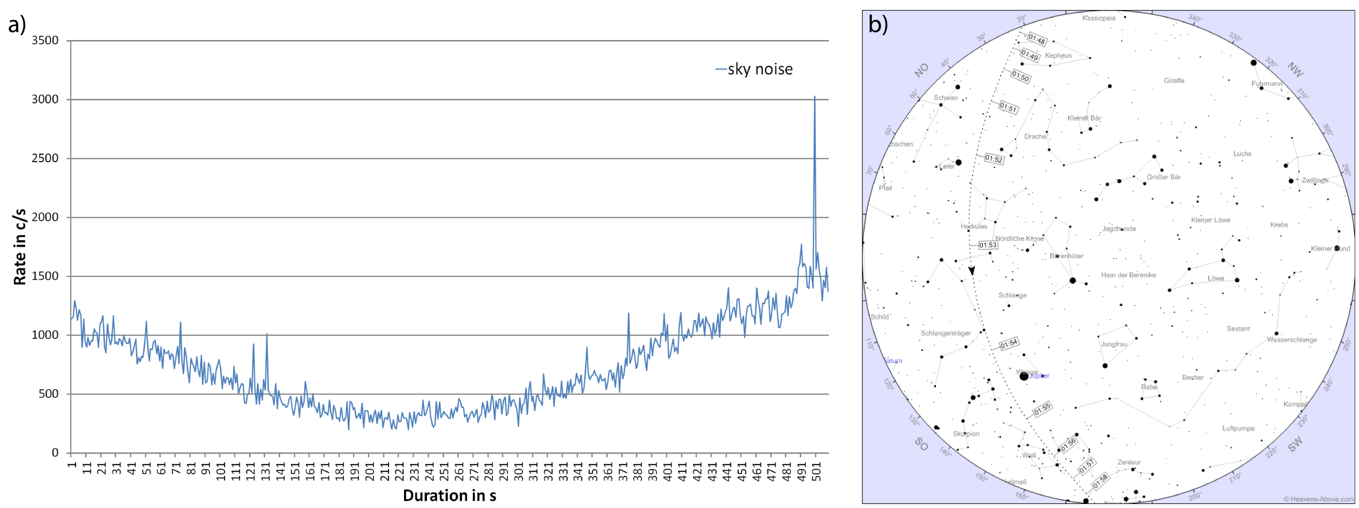

Supplementary Figure 1. a.) Background sky noise of a typical LEO satellite pass summed up over all 4 detectors. The count rate at the beginning and at the end of the pass is higher due to a higher observational air mass. The spikes originate from stars crossing the field of view of the detectors. Depicted in b.) is the satellite pass (Figure taken from www.heavens-above.com).

[1] Yin, J. *et al.* Satellite-based entanglement distribution over 1200 kilometers. *Science* **356**, 1140–1144 (2017).